Synthesis and Thermal Characterization of Phenolic Resin/Silica Nanocomposites Prepared with High Shear Rate-Mixing Technique

Maurizio Natali, Marco Monti, Josè Kenny, Luigi Torre

Department of Civil and Environmental Engineering, University of Perugia, Loc. Pentima Bassa 21, 05100 Terni, Italy

Received 9 July 2010; accepted 28 September 2010
DOI 10.1002/app.33494
Published online 23 December 2010 in Wiley Online Library (wileyonlinelibrary.com).

ABSTRACT: In this research the possibility to produce nanosilica/phenolic nanocomposites by means of a simple low labor cost mechanical approach was investigated. A commercial compatibilized nanosilica was selected as a filler and a resol diluted in methanol as a matrix. The morphology of the produced nanocomposites were studied by means of Scanning Electron Microscopy (SEM) and Transmission Electron Microscopy (TEM), whereas thermogravimetric analysis (TGA) was used to study the thermal stability of the nanocomposites. The post burning morphology of samples was also investigated. A rheological characterization was also carried out. The results of such study showed that it was possible to obtain a good degree of dispersion and distribution of the nanosilica particles, indicating that the proposed process could be successfully adopted as an alternative approach to sol-gel techniques. Thermogravimetric analyses showed that all the produced nanocomposites exhibited a better thermal stability than the pristine matrix. © 2010 Wiley Periodicals, Inc. J Appl Polym Sci 120: 2632–2640, 2011

Key words: nanocomposites; silicas; thermogravimetric analysis; thermosets

INTRODUCTION

Polymeric ablative composites play a strategic role in the aerospace field. They are used to produce thermal protection systems (TPSs), which are used to protect space vehicles from aerodynamic heating during the re-entry flight as well as to manufacture passively cooled rocket combustion chambers. This protective function is accomplished by a complex self-regulating heat and mass-transfer process known as ablation.[1] All the constituents of a polymeric ablative composite, the matrix, the fillers, and other additives actively participate to the ablation process.[2]

Phenolic resin is one of the most suitable and used matrix.[3] This is due to its high dimensional and thermal stability as well as to its remarkable thermal insulation and char retention.[4,5] To assist the char retention, fibrous reinforcements of carbon, silicon dioxide, refractory oxides, mineral asbestos, or glass have been added at the matrix. Properties of polymeric ablators have also been improved adding many kinds of inorganic particles, with the particle size ranging from the micrometric to the nanometric scale. Particularly, studies showed that micron-sized particles of silicon dioxide can significantly improve the ablative properties and the erosion resistance of the polymeric TPS.[1,6] In fact, when exposed to high temperature, silica particles form a very viscous-melted layer, which covers the ablated surface, forming a protective, antioxidizing film.[2]

The use of nanosilica also enabled the production of a new class of nanostructured composites. Phenolic resin/nanosilica hybrid composites have been successfully used in the field of high-temperature materials, for instance, as precursors of carbon/carbon composites. This class of nanocomposite is typically produced through sol–gel method,[7–9] that is, nanosilica particles are formed *in situ* using silicon-containing compounds like *tetra*-ethyl orthosilicate. Phenolic resin/silica hybrid nanocomposites are characterized by improved thermal properties and higher stiffness respect to the neat phenolic resin.[10] Furthermore, their use can improve the mechanical and thermal[11] properties of carbon/carbon composites as well as their oxidation resistance.[12]

The study of silica/phenolic nanocomposites is also very important, because such systems can be used in the preparation of silicon carbide particles. In fact, SiC is known to form via carbothermal reduction (high-temperature treatment in inert atmosphere) of solid-state carbon and gaseous silica.[13] If compared to other techniques, this process enables a simpler and cheaper production of SiC particles.[14]

Currently, no papers dealing with the preparation of silica/phenolic nanocomposites, directly produced by mixing the nanosilica with the liquid phenolic matrix, were found in literature, because the

Correspondence to: L. Torre (torrel@unipg.it).

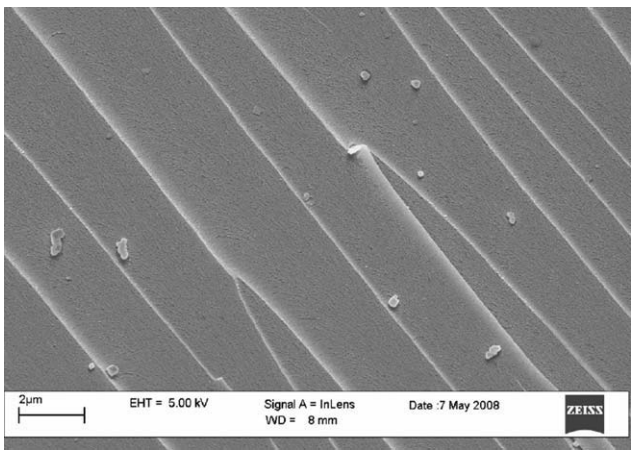

Figure 1 SEM image of a fracture surface referred to a neat resol sample prepared using the optimized curing cycle.

common approach is based on the sol–gel technique.[15] As a consequence, the study of the effects of nanosilica particles directly dispersed in a liquid phenolic matrix by means of a stirring technique, as a simpler and cheaper alternative approach to sol–gel processing, can be considered very interesting. Moreover, it was previously remarked that microsized silica particles dispersed in the phenolic matrix of a fiber-reinforced composites[16] are able to improve the ablative properties of the material. Thereby, in light of these considerations, the investigation of the use of nanosilica dispersed in a phenolic matrix, as a potential replacement of microsized silica, also results very important.

In our research, the processing, the morphology, and the thermal stability of silica/phenolic nanocomposites prepared in the above-mentioned way were studied. A liquid resol and a commercial compatibilized nanosilica (AEROSIL® R7200) were selected as raw materials. The morphology of obtained nanocomposites was examined by means of SEM and TEM analyses. Thermal stability of the produced materials was investigated by TGA, and then the postburning surface of sample was analyzed. To evaluate the effect of nanosilica on the processing characteristic, some rheological basic properties were studied.

EXPERIMENTAL

Materials and methods

The matrix chosen for the production of nanocomposite was a resol diluted in methyl alcohol, kindly provided by SHA (Germany). AEROSIL® R7200—a fumed silica, particularly an AEROSIL® 200, treated with a methacrylsilane (Evonik Degussa, Germany)—was used as nanosilica filler. AEROSIL® R7200 is characterized by a specific surface area equal to (150 ± 25)m^2/g, and the average primary particle size is 12 nm.

Nanocomposites were prepared using high-speed mixing. Two filler percentages were studied: 5% (resol : nanofiller, 95 : 5) and 20% (resol : nanofiller, 80 : 20). The first one can be considered as a common filler amount for this class of nanocomposites while the higher one was selected to test the behavior of the phenolic matrix when loaded at very high-filler percentages. It is worth to point out that this second percentage was chosen following the technical guidelines provided by AEROSIL® R7200 data sheet, which, although not related to phenolic matrices, suggests 20% as a limit filler load for this type of nanosilica.

Determination of the curing cycle of the neat resol

Even if phenolic resins are the oldest thermosetting polymers, their processing can be very difficult.[4] In fact, during the crosslinking process of phenolic matrices, the by-product of the polycondensation reaction is mostly water. As a consequence, defects such as voids and fractures can be formed during the cure. In our previous work,[17] we extensively discussed a method used to successfully produce defects free samples. To obtain high quality, voids free, and fractures free cured samples, it is of fundamental importance to delay the gelling of the resin and keeping the resol at a temperature of 60°C for a long time. A similar approach was successfully used by Kaynak et al.[18] The complete curing cycle can be summarized as follows: 120 h @ 60°C + 30 min @ 80°C + 30 min @ 100°C + 30 min @ 120°C + 30 min @ 140°C + 30 min @ 160°C + 30 min @ 180°C. According to our previous study, the final degree of cure resulted to be equal to 94.3%. Such processing time is much longer respect to curing cycles of other thermosetting polymers but is quite common for phenolic resins, for instance, in the production of carbon/phenolic ablators.[19]

To evaluate the effectiveness of the adopted curing cycle, a series of scanning electron microscopy analyses were performed on the cured specimens. A Zeiss Supra 25 SEM was used. Figure 1 shows a fracture surface of a specimen obtained curing the neat resol using the favorable temperature profile. The surface appeared without defects.

Preparation of the nanocomposites

To produce the nanocomposites, a high-speed mixer was used. In all cases, the blends were prepared according to the following procedure: the resin, as provided by the supplier (resol plus methanol), was weighted, and then the selected amount of nanofiller was added. During the mixing process, using a water jacket, the temperature of the metal bottle containing the blend was kept at a constant temperature

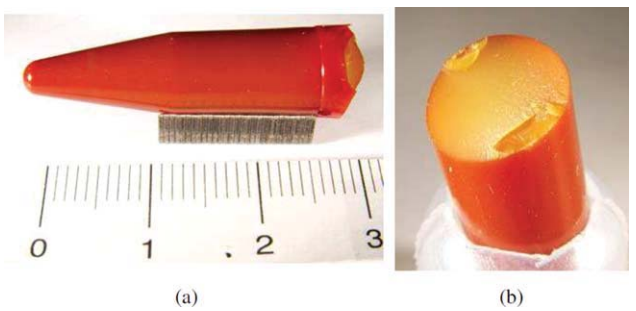

Figure 2 Characteristic appearance of a specimen prepared with the blend produced with 5% of nanosilica. (b) Refers to a fracture surface of this sample. No phase separation between matrix and the filler could be observed. [Color figure can be viewed in the online issue, which is available at wileyonlinelibrary.com.]

of 15°C. Such practice was necessary to minimize the evaporation of the methanol in which the resol was diluted. Even the production of the 20% nanosilica-loaded blend resulted to be user friendly, because the viscosity of this nanocomposite was low enough to ensure the cast ability of the blend. To further decrease the viscosity and improve the processability of the blends, a commercial viscosity reducer produced by Ewonik–Degussa (Dynasylan® 4144) was successfully used. It was added to the nanocomposite mixtures in a weight equal to 1% on the nanofiller concentration. For both filler percentages, the whole mixing time was of 2 h.

Finally, to remove the air trapped in the blends during mixing, they were left to sonicate for 10 h in a low-power ultrasonic bath (mod.AC-5, EMMEGI), and then they were degassed using a vacuum pump (about 5 min at a pressure of 20 mbar). Finally, the samples were prepared simply pouring the blends into the molds. To further lower the viscosity, the 20% wt blend was first heated at 40°C, and then it was poured in the mold.

Cure of nanocomposite samples

All nanocomposites were cured using the temperature profile applied at the neat resol and mentioned in the previous section. To understand the effect of this curing cycle on the morphology of cured materials, optical analyses were carried out on a fracture surface of the specimens. Several authors used a similar methodology. Kaynak et al.[18] showed how long curing cycles can easily promote phase separation between the matrix and the nanofiller. According to optical analyses performed on produced nanocomposites, although our temperature profile was characterized by a very long residence time under the gel point, this solution did not produce any phase separation between the nanofiller and the matrix. Moreover, optical analyses also evidenced that all nanocomposite samples exhibited no presence of voids or fractures, meaning that the cure cycle used for the preparation of the neat resol specimens could be successfully applied to nanocomposites. Pictures referred to specimens prepared with the two produced nanocomposites are showed in Figure 2(a,b) (referred to 5% loaded blends) and Figure 3(a,b) (related to 20% loaded material).

Rheological characterization

To improve the processing of the nanocomposites as well as to investigate the chemical–physical interaction between the matrix molecules and the nanosilica particles, the rheological properties of the produced blends were studied. Particularly, the complex viscosity of the pristine resol and of the nanocomposites was examined. All tests were performed with a rotational rheometer (Rheometric Scientific model ARES N2) using a parallel-plate geometry. Dynamic tests were carried out with an oscillation frequency growing from (0.01 to 100) rad/s. Measurements were performed at temperature of 25°C and to keep the response in the linear viscoelastic range, a strain equal to 3% was applied.

SEM characterization

The dispersion of the nanosilica particles in the studied nanocomposites was evaluated using scanning electron microscopy. A Zeiss Supra 25 was used.

TEM characterization

The morphology of the nanocomposites was further studied using transmission electron microscopy (Philips EM 208). Samples were prepared by ultramicrotomy at room temperature, producing sheets of ~ 200-nm thick. No further procedures were used to enhance the contrast.

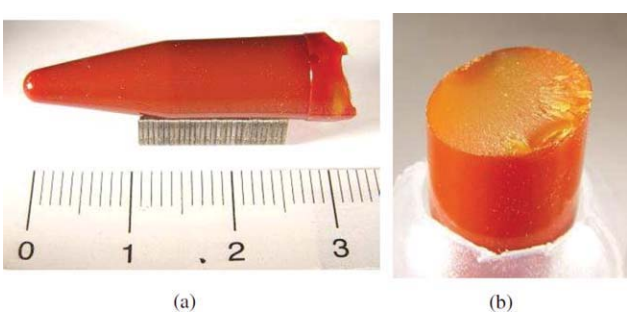

Figure 3 Typical specimen prepared with the blend produced at 20% of nanosilica amount. (b) Shows a fracture surface of this sample. Also in this case, no phase separation between matrix and the filler could be observed. [Color figure can be viewed in the online issue, which is available at wileyonlinelibrary.com.]

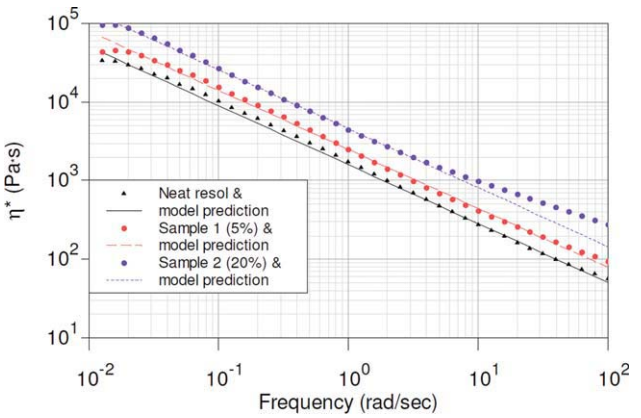

Figure 4 Complex viscosity of the neat resin and nanocomposites as a function of frequency. [Color figure can be viewed in the online issue, which is available at wileyonlinelibrary.com.]

Thermogravimetric analysis

Thermal stability of the produced nanocomposites was studied by means of thermogravimetric analysis (TGA). A very good experimental repeatability was obtained milling the nanocomposite samples. A narrow particle diameter distribution was used, with the mean particle size of about 200 μm. Samples of about (10 ± 1) mg were characterized. For the same purpose, TGA analysis on each material was performed at least 10 times. The measurements were performed both in air as well as in nitrogen, applying a linearly growing temperature ramp (the heating rate was of 20°C/min). Measurements were performed on a Seiko Exstar 6000 TGA. The results obtained in air were most suitable to describe the behavior of the studied material when referred to an oxidative environment. Conversely, measurements performed in nitrogen were most appropriate to describe the behavior of the material when referred to a nonoxidative environment.

RESULTS AND DISCUSSION

Rheological characterization

The complex viscosity of the pristine resol and nanocomposites was examined. Figure 4 shows the dynamic viscosity η* as a function of frequency.

According to experimental results, in the whole range of analyzed frequencies, the neat resol exhibits a sharp shear-thinning behavior, a typical response for this kind of liquid resols. At all filler percentages, the introduction of nanosilica did not modify the shear-thinning tendency exhibited by the pristine matrix. In quantitative terms, the introduction of silica nanoparticles increased the viscosity, but, if compared to other kind of nanofillers, also the introduction of 20% of nanosilica did not produce a very large increase of η*. In the whole range of frequencies, the gap between the dynamic viscosity pattern of the neat matrix and the corresponding curve referred to 5% loaded nanocomposite always remained constant. Concerning the 20% loaded blend, this gap is nearly constant up to a frequency of about 1 rad/s. Starting from this value of frequency, this gap tended to increase slightly.

Experimental data were fitted using a power-law-like model $\eta^* = K\,\omega^{n-1}$. Table I summarizes the value for K and n for all studied materials.

It is possible to see that a value of n equal to 0.25 is able to fit the trend of η* as a function of frequency, both for neat resol as well as for low-loaded nanocomposite. Only for the 20% loaded blend, above a frequency of about 1 rad/s, it is possible to identify a difference between the model and the experimental data.

Morphological analysis

SEM characterization

To better understand the morphology of the cured nanocomposites, SEM analyses were carried out on the fracture surface of samples produced with these materials. The SEM surface referred to the neat resol (Fig. 1) was used as a reference.

Concerning the morphology of produced materials, 5% loaded nanocomposite [Fig. 5(a,b)] showed a nearly smooth surface in which there were embedded nodules of ~ 200 nm diameter. A similar morphology was identified by Zhang et al.[20] for epoxy-based nanocomposites loaded with nanosilica particles. Increasing the filler load (20% weight), a highly wrinkled nodular structure could be observed in the samples [Fig. 6(a,b)]. Moreover, analyses carried out at the higher magnification evidenced a morphology in which the dimension of nodules was compatible with the mean diameter of the used nanosilica, that is, smallest nodules visible in the Figure 6(b) are nanosilica particles attached to the matrix. At a similar filler percentage, studying a poly(methyl methacrylate) system loaded with nanosilica, Garcia et al.[21] found a morphology very similar to 20% loaded system produced in this research.

Finally, SEM images showed that all the produced nanocomposites did not exhibit any presence of voids or defects, confirming that the curing cycle

TABLE I
Coefficients of the Power-Law-Like Model for Both the Neat Resol as Well as the Nanocomposites

	Neat resol	5%-loaded nanocomposite	20%-loaded nanocomposite
K (Pa s^n)	1600	2500	4600
N	0.25	0.25	0.25

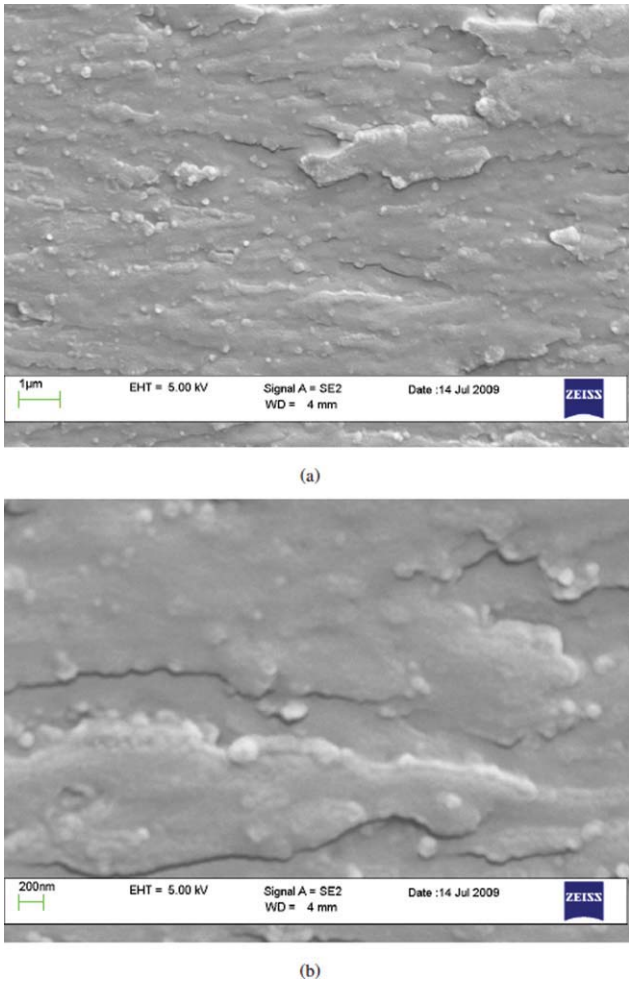

Figure 5 SEM images related to a fracture surface of 5% loaded nanosilica composite. [Color figure can be viewed in the online issue, which is available at wileyonlinelibrary.com.]

applied to polymerize the neat matrix yields good quality samples also for nanocomposites.

TEM characterization

TEM analysis was performed on produced nanocomposites. Results can be summarized as follows. Regarding 5% loaded nanocomposite, TEM images showed a very good degree of dispersion as well as an homogeneous distribution of nanosilica particles [Fig. 7(a)]. Smallest dots visible in this image are clearly single nanosilica particles. Nanosilica particles easily tend to aggregate each other, and, decreasing the diameter of the particles, the degree of agglomeration typically increases.[22] Comparing our work to other researches, involving the use of nanosilica dispersed in a thermosetting matrix by means of mechanical stirring, the obtained degree of dispersion could be considered satisfactory.[23,24] In fact, samples produced using 5% loaded blends showed at worse zones in which there were cluster of nanosilica particle with an average dimension of about 200 nm [Fig. 7(b)].

Concerning the 20% wt blend, also in this case, the dispersion and the distribution of the filler could be considered good, especially if we take into account the high loading of filler. In Figure 8(b), single nanosilica particles were clearly distinguishable. Concluding, as it has been pointed out by SEM analysis at both filler percentages, TEM results confirmed the good dispersion and distribution of the nanosilica particles.

Thermogravimetric analysis

Results in nitrogen

Figure 9(a,b), respectively, shows that TGA and DTG patterns of the neat resol and the nanocomposites performed in nitrogen environment. Under TGA test conditions, the neat matrix initially undergoes charring, and the endothermic cracking of the organic phase liberates gaseous products. Water is the principal product up to about 350°C; depolymerization then occurs, with release of phenol and larger

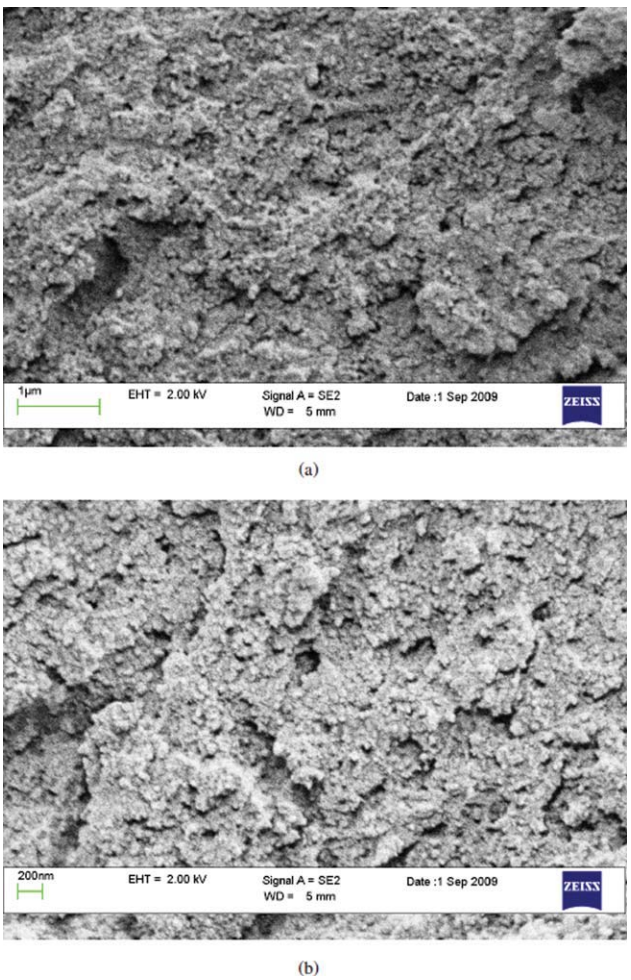

Figure 6 SEM image of a fracture surface of 20% loaded nanocomposite. The clearly distinguishable granular morphology is directly related to nanosilica particles embedded in the matrix. [Color figure can be viewed in the online issue, which is available at wileyonlinelibrary.com.]

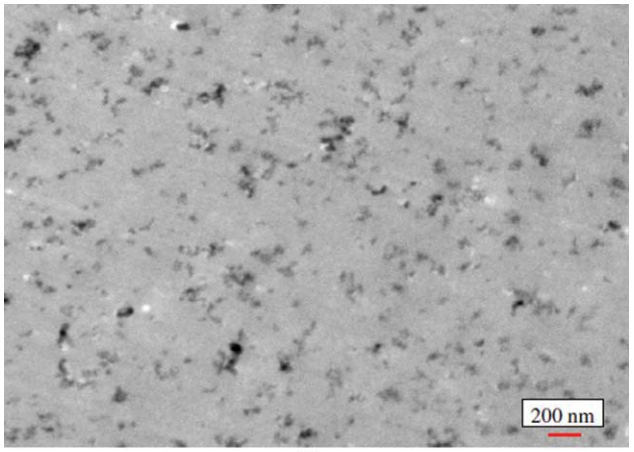

(a)

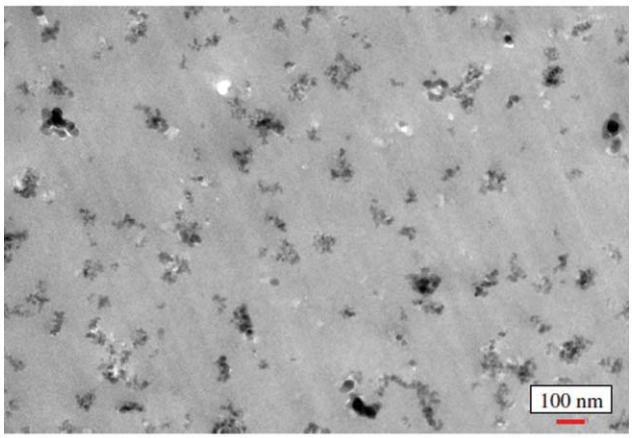

(b)

Figure 7 Representative TEM images referred to 5% loaded blends. A very good degree of dispersion of nanosilica particles was obtained. Even in the worst conditions, no nanosilica clusters greater than approximately 200 nm could be detected (b). [Color figure can be viewed in the online issue, which is available at wileyonlinelibrary.com.]

species; above ~ 400°C, lower molecular weight products are evolved, with H_2 as the primary product (in absence of oxygen) at 700°C and above.[25]

TGA/DTG thermograms showed that both nanocomposites always exhibited a superior thermal stability than the neat resol. At all temperatures, degradation rate trends of nanocomposites always exhibited a lower velocity than the pristine matrix. Particularly, the higher was the filler amount, and the smaller was the degradation rate exhibited by the material. The char yield of the nanocomposites increased with the nanosilica content (Table II). Increasing the char retention, the introduction of nanosilica hindered the production of gaseous product.[26]

The first peak in the DTG patterns centered at ~ 80°C can be attributed at the release of water. However, the extent of this peak is merely due to the evaporation of the water absorbed by the powders of cured materials before to be tested in the TGA. In fact, due to the high degree of cure reached at final stage of the selected cure profile (~ 94% for neat resol), the first peak in the DTG patterns cannot be associated to an uncompleted curing of materials. Finally, for all materials, the main DTG peak can be associated to the release of gas due to pyrolysis of the matrix.[27,28]

Defining the temperature of the maximum degradation rate as T_{max}, which is the temperature at which the derivate of the weight W with respect to T is maximum, experimental results showed that, in no cases, nanosilica affected the value of this variable. In fact, both for neat resol as well as for nanocomposites, the value of T_{max} resulted to be equal to ~ 560°C.

Results in air

TGA measurements performed on the studied material under oxidizing conditions [Fig. 10(a)] showed

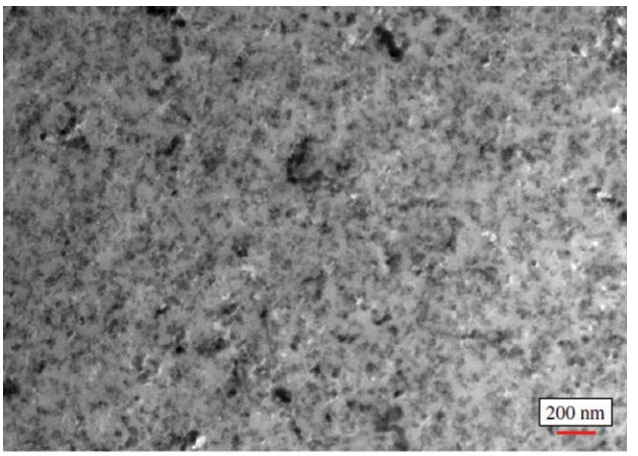

(a)

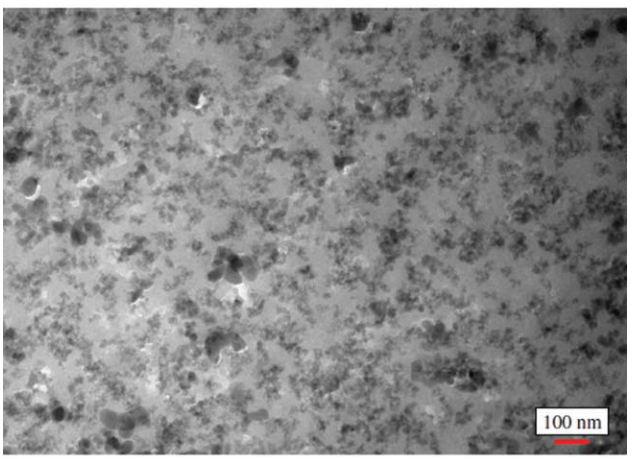

(b)

Figure 8 TEM images produced on 20% loaded blend. Even in this case, especially considering the high filer concentration, a good degree of dispersion and distribution of nanoparticles was achieved. Increasing the magnification, it was possible to identify single nanosilica particles, confirming the effectiveness of the mixing technique even at this high filler concentration (b). [Color figure can be viewed in the online issue, which is available at wileyonlinelibrary.com.]

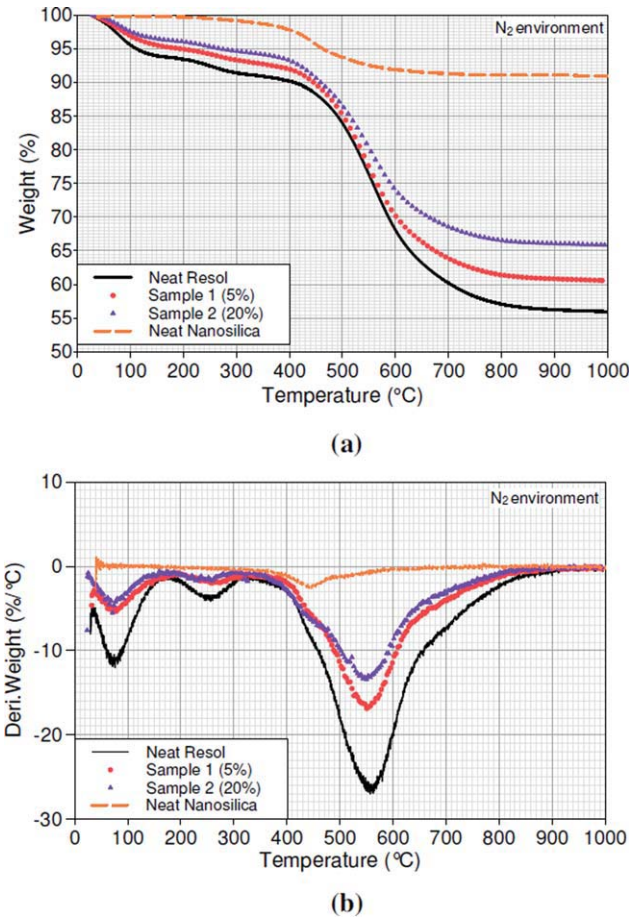

Figure 9 TGA (a) and DTG (b) curves performed in nitrogen on the neat resol and nanocomposites. According to the results, all nanocomposites showed a superior thermal stability than the pristine matrix. [Color figure can be viewed in the online issue, which is available at wileyonlinelibrary.com.]

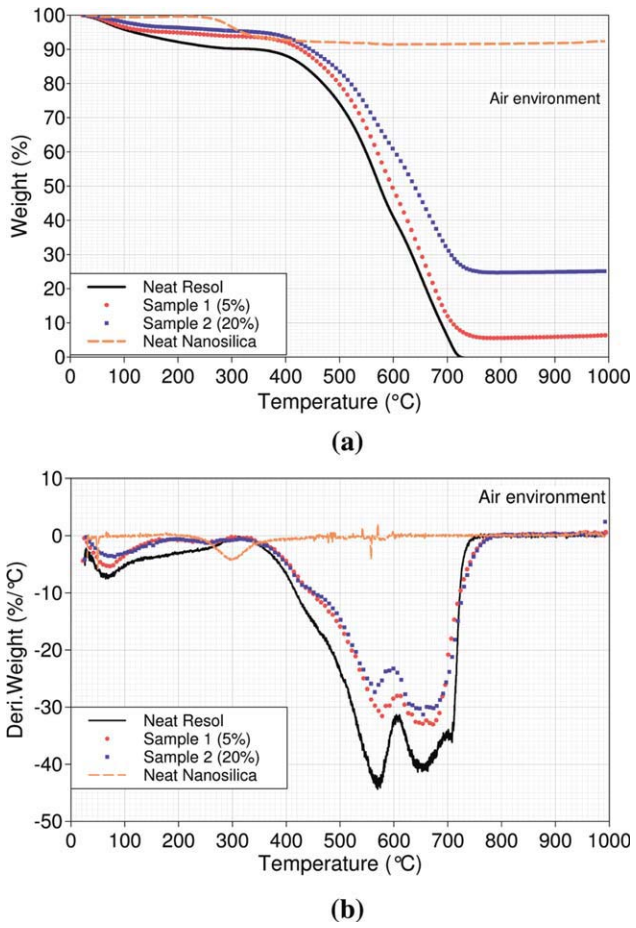

Figure 10 TGA (a) and DTG (b) measurements performed in air on the neat resol and nanocomposites. All nanocomposites exhibited an increased thermal stability than the neat matrix. [Color figure can be viewed in the online issue, which is available at wileyonlinelibrary.com.]

that all nanocomposites always exhibited a superior thermal stability respect to the pristine resol. After 750°C, the pristine resol was completely burned, because, beyond this temperature, no weight loss could be observed. On the other hand, in the case of both nanocomposites, TGA patterns showed that, up to a temperature of ~ 780°C, the thermal stability was significantly improved. Another indication of the improved thermal stability induced by the use of nanosilica came from the evaluation of the $T_{10\%}$ temperature (representing the temperature at which a 10% of mass loss is reached) and the $T_{50\%}$, which is the same parameter evaluated at a 50% of loss of weight. Both these temperatures well showed the remarkable effect of nanosilica on the thermal stability of matrix. Table III summarizes such results.

Concerning the composition of the residual mass of studied materials, because, after 750°C, the neat matrix was completely burned, and the residual masses of nanocomposites could be only composed by the nanosilica itself. However, for both nanocomposites, the filler-to-matrix ratio at the end of the measurement process resulted to be higher than the original ratio. Such situation can be completely justified considering that, after curing, the matrix

TABLE II
Residual Mass of the Tested Materials After TGA Analysis in Nitrogen Environment

	Neat resol	5%-loaded nanocomposite	20%-loaded nanocomposite
$T_{10\%}$ (°C)	344.6	427.8	445.8
$T_{50\%}$ (°C)	574.4	597.3	638.9

TABLE III
$T_{10\%}$ and $T_{50\%}$ Temperatures for the Neat Resol and the Nanocomposites Tested in Air Atmosphere

	Neat resol	5%-loaded nanocomposite	20%-loaded nanocomposite
Residual char mass (%)	52.3	61.2	72.1

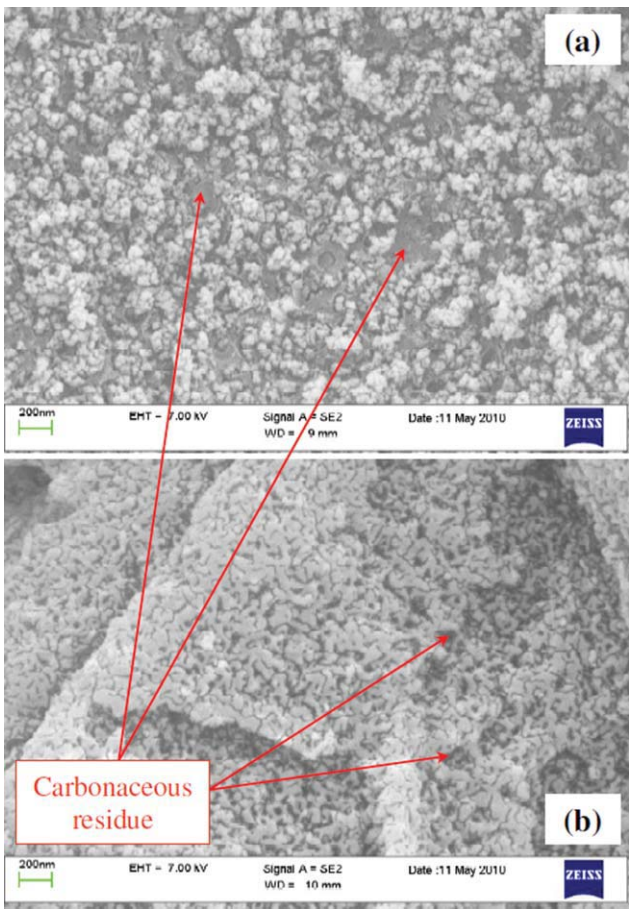

Figure 11 Morphology of the nanocomposites after TGA scan in nitrogen: (a) 5% and (b) 20% loaded blend. [Color figure can be viewed in the online issue, which is available at wileyonlinelibrary.com.]

experienced a well-predictable mass reduction due to methanol evaporation, therefore leading to a higher filler/matrix ratio. In fact, according to resin data sheet, the resole has a solid content of about 70%. For the nanocomposites tested in air, the complete removal of the organic matrix, due to the high-temperature exposure in an oxidative environment, hindered any possibility to produce organosilicon compounds. In fact, the formation of such structures, which works as flame retardants for polymeric materials,[29–31] is enabled only when a carbothermal reduction between silica and carbon is allowed.

Finally, concerning the DTG curves obtained in air, it is possible to observe that the typical single bell-shaped DTG patterns obtained in the nitrogen environment, in the presence of the oxidative atmosphere, turned into a two-peak curves. Besides the first main peak centered at $\sim$ 560°C, it appeared another peak of comparable intensity, centered at a temperature of $\sim$ 650°C. This secondary peak can be related at the loss of mass due to the combustion processes due to the interaction of the matrix with the oxygen contained in the air. Finally, the degradation rate of the higher loaded blend was always smaller or, at worse, comparable to the value displayed by 5% loaded nanocomposite. Also, in the case of TGA tests performed in oxidative environment, the higher was the filler amount, and the smaller was the degradation rate experienced by the nanocomposites.

Morphology of post burning surfaces

To perform a morphological study of the postburning surfaces of produced nanocomposites, bulk samples of these materials were exposed to the same TGA scans previously mentioned. Schartel et al.[32] used a similar study to investigate the burned residue of layered silicate epoxy nanocomposites. Figure 11(a) shows the postburning surface of 5% loaded nanocomposite while Figure 11(b) is referred to 20% loaded matrix, after a TGA scan in nitrogen. The darker zones in the pictures are composed by the carbonaceous residue of the matrix. Energy dispersive X-ray spectroscopy (EDX) analysis confirmed a strong presence of the carbon element in these areas

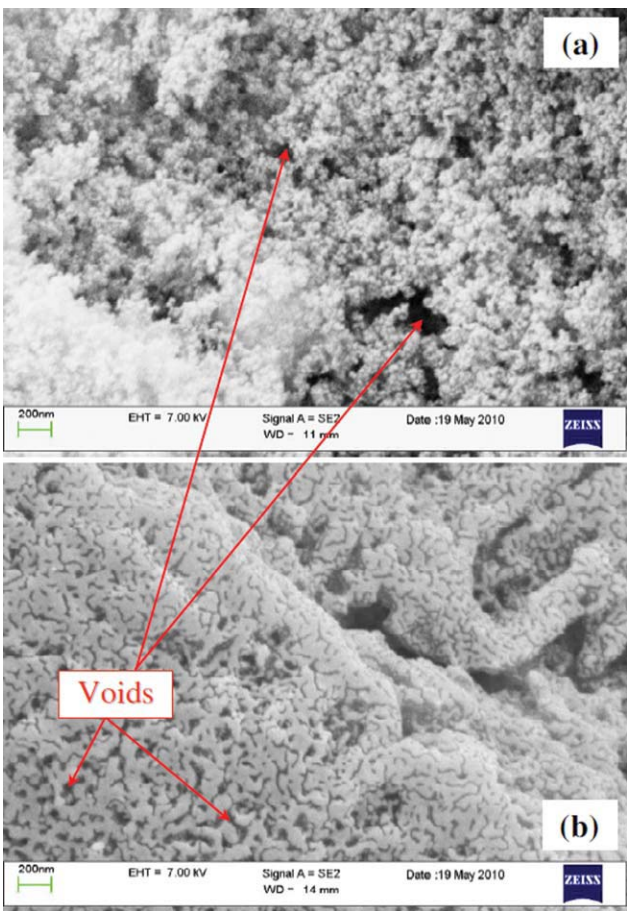

Figure 12 Morphology of the nanocomposites after TGA scan in air: (a) 5% and (b) 20% loaded blend. [Color figure can be viewed in the online issue, which is available at wileyonlinelibrary.com.]

of the burned samples. Moreover, the typical appearance of burned samples, with their dark color, clearly evidenced the presence of carbon. This result confirmed that, at the temperature existing near the charred surface, in a nonoxidizing environment, the reaction, which produces silicon carbide, is not hindered. SEM analysis also showed that, after the TGA scan, nanosilica particles sintered. In fact, it is not possible to observe any isolated particle, confirming that these particles have undergone sintering.[32]

Figure 12(a,b) is referred to burned surfaces of nanocomposites tested in air. In this case, the high-temperature treatment in an oxidizing environment completely removed the organic matrix: the darker zones of these pictures are merely empty spaces. As a consequence, after burning in air, the nanocomposites morphology converted in a carbon-free skeleton structure, formed by sintered nanosilica particles. EDX results confirmed the absence of carbon. In this case, the appearance of burned samples, with their typical pure white color, clearly evidenced the presence of silica alone.

CONCLUSIONS

In this research, it has been shown that phenolic resin/silica hybrid nanocomposites can be successfully produced by means of a high-speed stirring technique as a simpler and cheaper approach to sol–gel processing. This research evidenced that, at all studied filler percentages (5 and 20%) to effectively produce a well dispersed and defects free nanocomposite with casting capability, it was necessary to use high-speed mixing followed by a final outgassing step. Low-power sonication resulted to be a very effective practice to promote removal of air trapped during the stirring step. According to SEM and TEM analyses, at all studied filler percentages, the nanosilica particles were well distributed and dispersed into the matrix. Thermogravimetric analyses carried out in nitrogen as well as in air showed that the use of nanosilica improved the thermal stability of the pristine resol. Both in nitrogen as well as in oxidizing environment, the thermal stability of the matrix increased with the increase of the filler load. The morphology of the postburning surfaces of samples was also studied after the TGA characterization. The analysis evidenced that, under oxidizing conditions, the organic matrix was completely removed, and the nanocomposite structure converted in a carbon-free skeleton due to the sintering process of nanosilica. On the other hand, in a nonoxidizing environment, the charred residue of the organic matrix was not removed and so enabling the possibility to produce silicon carbide structures.

References

1. D'Alelio, G. F.; Parker, J. A. Ablative Plastics; Marcel Dekker: New York, 1971.
2. Miller, G. H.; Robinson, G. C. Jr. Investigation of Fiber Systems of Ablative Materials, NASA CR-54722 TEI-TP 25, September 1965.
3. Knop, A.; Scheib, W. Chemistry and Application of Phenolic Resins; Springer-Verlag: Berlin, 1979.
4. Kuzak, S. G.; Hiltz, J. A.; Waitkus, P. A. J Appl Polym Sci 1998, 67, 349.
5. Firouzmanesh, M. R.; Azar, A. A. J Appl Polym Sci 2003, 88, 2455.
6. Peterson, D. A.; Winter, J. M.; Shinn, A. M. Jr. Rocket Engine Evaluation of Erosion and Char as Functions of Fabric Orientation for Silica-Reinforced Nozzle Materials, NASA TM X-1721, January 1969.
7. Lin, J. M.; Ma, C. C. M. Polym Degrad Stab 69, 2, 12 July 2000, 229–235.
8. Haraguchi, K.; Usami, Y.; Ono, Y. J Mater Sci 1998, 33, 3337.
9. Haraguchi, K.; Usami, Y.; Yamamura, K.; Matsumoto, S. Polymer 1998, 39, 6243.
10. Ma, C. C. M.; Lin, J. M.; Chang, W. C.; Ko, T. H. Carbon 2002, 40, 977.
11. Lin, J. M.; Ma, C. C. M.; Tai, N. H.; Chang, W. C.; Tsai, C. C. Polym Compos 2000, 21, 305.
12. Lin, J. M.; Ma, C. C. M.; Chang, W. C. J Mater Sci 2001, 36, 4259.
13. Weimer, A. W.; Nilsen, K. J.; Cochran, G. A.; Roach, R. P. AIChE J 1993, 39, 493.
14. Jung, Y. S.; Kwon, O. J.; Oh, S. M. J Am Ceram Soc 2002, 85, 2134.
15. Zou, H.; Wu, S.; Shen, J. Chem Rev 2008, 108, 3893.
16. Richter, G. P.; Smith, T. Ablative material testing for low-pressure, low-cost rocket engines, 32nd Combustion Subcommittee, Propulsion Systems Hazards Subcommittee, 22nd Exhaust Plume Technology Subcommittee, and 4th SPIRITS User Group Joint Meeting, Huntsville, AL, United States, 23–27 October 1995.
17. Natali, M.; Kenny, J. M.; Torre, L. Compos Sci Technol 2010, 70, 571.
18. Kaynak, C; Tasan, C. C. Eur Polym J 2006, 42, 1908.
19. Pulci, G.; Tirillò, J.; Marra, F.; Fossati, F.; Bartuli, C.; Valente, T. Compos A 2010, 41, 1483.
20. Zhang, H.; Zhang, Z.; Friedrich, K.; Eger, C. Acta Mater 2006, 54, 1833.
21. Garcìa, N.; Corrales, T.; Guzmàn, J.; Tiemblo, P. Polym Degrad Stab 2007, 92, 635.
22. Goertzena, W. K.; Kessler, M. R. Compos A: Appl Sci Manuf 2008, 39, 761.
23. Battistella, M.; Cascione, M.; Fiedler, B.; Wichmann, M. H. G.; Quaresimin, M.; Schulte, K. Compos A 2008, 39, 1851.
24. Goertzen, W. K.; Sheng, X.; Akinc, M.; Kessler, M. R. Polym Eng Sci 2008, 48, 875–883.
25. Svkes, G. F. NASA TN D-3810, National Aeronautics and Space Administration, February 1967.
26. Chiang, C. L.; Ma, C. C. M. Polym Degrad Stab 2004, 83, 207.
27. Puglia, D.; Kenny, J. M.; Manfredi, L. B.; Vazquez, A. Mater Eng 2001, 12, 55.
28. Manfredi, L. B.; Puglia, D.; Tomasucci, A.; Kenny, J. M.; Vazquez, A. Macromol Mater Eng 2008, 293, 878.
29. Wu, C. S.; Liu, Y. L.; Chiu, Y. S. Polymer 2002, 43, 4277.
30. Wang, W. J.; Perng, L. H.; Hsiue, G. H.; Chang, F. C. Polymer 2000, 41, 6113.
31. Zheng, S.; Wang, H.; Dai, Q.; Kuo, X.; Ma, D.; Wang, K. Makromol Chem Phys 1995, 196, 269.
32. Schartel, B.; Weiβ, A.; Sturm, H.; Kleemeier, M.; Hartwig, A.; Vogt, C.; Fischer, R. X. Polym Adv Technol 2010, DOI: 10.1002/pat.1644.